MATHEMATICS AND COMPUTATIONAL SCIENCES

Vol 6(1), 2025, pp:1-18

DOI:10.30511/mcs.2025.2046047.1257

ISSN:2717-2708

http://mcs.qut.ac.ir/

Qom University of Technology

Numerical approximations for damped wave equation with Neumann boundary conditions

Mohammed Homod Hashim [1], **Sattar M. Hassan** [2], **Ayat A. Hameed** [3], **Akil J. Harfash** [4]

[1,3,4]Department of Mathematics, College of Sciences, University of Basrah, Basrah, Iraq

[2]Department of Mathematics, College of Education, University of Misan, Misan, Iraq

Abstract: This research paper investigates the numerical analysis of the damped wave equation (DWE), focusing on the properties of numerical solutions achieved via semi-discrete approximation (SDA) and fully-discrete approximation (FDA) finite element methods (FEMs). This study established the existence of SDA and FDA solutions. Theoretical results are validated with numerical examples conducted in one, two, and three dimensions, demonstrating the accuracy and effectiveness of the proposed approaches.

Keywords: Finite element; Wave equation; Weak solution; Semi-discrete approximation; Fully-discrete approximation.

2020 Mathematics Subject Classification: 65M60; 65M12; 35D30

Receive: 18 November 2024, **Accepted:** 06 January 2025

1 Introduction

This article examines the Cauchy problem for the semilinear wave equation as outlined in references [4]:

$$\gamma_{tt} + \gamma_t - \Delta\gamma + \gamma^3 = 0, \qquad \text{in} \quad \Psi \times [0,T], \tag{1.1}$$

$$\frac{\partial\gamma}{\partial\nu} = 0, \qquad \text{on} \quad \partial\Psi \times [0,T], \tag{1.2}$$

$$\gamma(\cdot,0) = \gamma_1^0, \qquad \gamma_t(\cdot,0) = \gamma_2^0 \qquad \text{in} \quad \Psi. \tag{1.3}$$

where Ψ is an open bounded domain in $\mathbb{R}^\ell$, $\ell \geq 1$ with a smooth boundary $\partial\Psi$, γ is the displacement of the wave field, and ν represents the outward unit normal to $\partial\Psi$.

Because it models the energy dissipation in systems exposed to wave dynamics, DWE is essential to many scientific and engineering fields. A damping factor is added to this equation, which is an extension of the classical wave equation, to account for the gradual decrease in wave amplitude. It is important for applications where knowledge of stability, energy loss, and the asymptotic behaviour of systems is essential. DWE's asymptotic behaviour, in which solutions eventually converge to heat-type equations, is a key component of its significance. It shows how energy dissipation converts wave-like behaviour into diffusive dynamics in a variety of contexts, including Euclidean space

[1]mohammed.hmmod@uobasrah.edu.iq

[2]star.mozan@yahoo.com

[3]ayat.abdulkareem@uobasrah.edu.iq

[4]Corresponding author: akil.harfash@uobasrah.edu.iq

[41]. Additionally, the severely damped scenario reduces spectral abscissa, which is crucial for regulating spectral behaviour under perturbations and conducting stability analyses [10].

DWE is essential in real-world applications for systems with vibrating components, including suspension bridges, where damping prevents catastrophic resonance and stabilizes oscillations by taking energy loss over time into account [45]. Engineers may create boundary conditions and control techniques that maximize energy consumption by applying this approach to radial wave equations, where controllability becomes crucial [44]. Determining the lifespan of solutions in dynamic contexts is impacted by DWE, which also helps to explain complicated phenomena like blow-up behaviour in nonlinear, time-dependent scenarios [37]. It is also crucial for applications like fluid dynamics and material sciences that need strict control over boundary conditions because of its involvement in global stability and convergence rates [16].

Researchers may simulate and comprehend wave behaviour in a variety of dampening conditions by employing numerical solutions to the DWE. These techniques are particularly helpful for examining the stability, oscillation, and decay rates of solutions all of which are important for applications such as material science, mechanical system design, and seismic wave modeling. For example, in seismic investigations, scientists may forecast wave attenuation in various geological strata employing numerical models, which helps with earthquake impact assessment and mitigation. Finite difference, finite element, and spectral approaches are some common numerical techniques for resolving the DWE. While each approach has its own merits, finite difference techniques are frequently employed due to their simple discretisation schemes, while FEMs give more flexibility when dealing with complicated geometries and boundary conditions. For further information on the numerical solutions for the DWE, see, for example, [36, 39, 42]. The mathematical ideas and computer methods that enable precise and efficient numerical modeling of damped wave events are highlighted in these sources.

Many researchers have extensively studied the semilinear wave equation in the literature [35, 5, 29, 40], with investigations into the global existence and other characteristics of equations (1.1)-(1.3) documented in [43, 46]. Numerical approaches to the nonlinear wave equation have also been widely explored. Numerous effective and precise numerical methods have been developed, including continuous Galerkin methods [33, 9], discontinuous Galerkin methods [32, 17, 34], and mixed finite element techniques [31]. Recently, there has been growing interest in finite difference schemes for wave equations [12, 13, 38, 28]. In particular, in [14, 11], finite difference schemes of various accuracy orders have been presented. This study aims to examine two finite difference-based numerical schemes for the semilinear wave equations (1.1)-(1.3).

It is important to highlight that previous numerical studies addressing the DWE did not focus on theoretically analyzing the numerical solutions, particularly regarding solution spaces and stability bounds. A detailed examination of the numerical approximation will be performed, which includes identifying the numerical solution spaces.

To develop our approach, we observe that with the transformation $\xi = \gamma_t + \gamma$, the system (1.1)-(1.3) transforms into:
(Θ) Find $\{\gamma, \xi\}$ such that

$$\xi_t - \Delta\gamma + \gamma^3 = 0, \qquad \text{in} \quad \Psi \times [0,T], \tag{1.4}$$

$$\xi = \gamma_t + \gamma, \qquad \text{in} \quad \Psi \times [0,T], \tag{1.5}$$

$$\frac{\partial\gamma}{\partial\nu} = 0, \qquad \text{on} \quad \partial\Psi \times [0,T], \tag{1.6}$$

$$\gamma(\cdot,0) = \gamma_1^0, \qquad \xi(\cdot,0) = \gamma_1^0 + \gamma_2^0 := \xi^0, \qquad \text{in} \quad \Psi. \tag{1.7}$$

Next, we present a weak formulation of the system (1.4) and (1.5) in the form:
(Θ) Find $\gamma(.,t), \xi(.,t) \in H^1(\Psi)$ such that $\gamma(.,0) = \gamma^0(.), \xi(.,0) = \gamma_1^0(.)$ and for almostevery $t \in (0,T)$,

$$(\xi_t, \mu) + (\nabla\gamma, \nabla\mu) + (\gamma^3, \mu) = 0, \qquad \text{in} \quad \Psi \times [0,T], \tag{1.8}$$

$$(\gamma_t, \mu) + (\gamma, \mu) = (\xi, \mu), \qquad \text{in} \quad \Psi \times [0,T]. \tag{1.9}$$

This passage describes the structure of the paper. Section 2 presents the notation employed throughout the study. Section 3 addresses the SDA of Problem (Θ), with a focus on global existence presented in Section 3.1. FDA of Problem (Θ) is discussed in Section 4, where stability bounds are also established. Section 4.1 examines the existence of FDA. Finally, Section 5 details a numerical algorithm for implementing the FDA of Problem (Θ) and includes numerical error calculations.

2 Finite element spaces and associated results

Let $\Im^{\hbar}$ represent a finite element space, which is a subspace of $H^1(\Psi)$, and is defined as follows:

$$\Im^{\hbar} := \{\varepsilon \in C(\overline{\Psi}) : \varepsilon|_{\tau} \text{ is linear } \forall \tau \in \mathcal{T}^{\hbar}\}.$$

The set $\{\kappa_j\}_{j=1}^{J}$ defines the standard basis functions for $\Im^{\hbar}$, fulfilling the condition $\kappa_j(\varsigma_i) = \delta_{ij}$ for each $i, j = 1, \ldots, J$. Here, $\mathcal{N}^{\hbar} := \{\varsigma_j\}_{j=0}^{J}$ represents the collection of nodes associated with the partition $\mathcal{T}^{\hbar}$. Moreover, we present that:

$$\begin{aligned}\Im^{\hbar}_{\geq 0} &:= \{\varepsilon \in \Im^{\hbar} : \varepsilon(\varsigma_j) \geq 0, j = 0, ..., J\}\\ &\subset H^1_{\geq 0} := \{\varepsilon \in H^1(\Psi) : \varepsilon \geq 0 \ a.e. \in \Psi\}.\end{aligned}$$

The operator $\pi^{\hbar} : C(\overline{\Psi}) \to \Im^{\hbar}$ denotes the Lagrange interpolation operator, also known as the piecewise linear interpolant. This operator guarantees that:

$$\pi^{\hbar}\varepsilon(\varsigma_j) := \varepsilon(\varsigma_j), \quad \text{for } \ j = 0, ..., J.$$

Additionally, we define a discrete L^2 inner (or semi-inner) product on $\Im^{\hbar}(C(\overline{\Psi}))$ as follows:

$$(u, v)^{\hbar} := \int_{\Psi} \pi^{\hbar}(u(\mathbf{x})v(\mathbf{x}))d\mathbf{x} = \sum_{j=1}^{J} \widehat{M}_{jj}\ u(\varsigma_j)\, v(\varsigma_j). \tag{2.1}$$

where $\widehat{M}_{jj} = (\kappa_j, \kappa_j)^{\hbar} = (1, \kappa_j) > 0$. By observing (2.1), it is straightforward to confirm that:

$$(\varepsilon_1, \varepsilon_2)^{\hbar} = (\pi^{\hbar}\varepsilon_1, \varepsilon_2)^{\hbar} = (\pi^{\hbar}\varepsilon_1, \pi^{\hbar}\varepsilon_2)^{\hbar} \quad \forall \varepsilon_1, \varepsilon_2 \in C(\overline{\Psi}). \tag{2.2}$$

In the finite element space $\Im^{\hbar}$, several key results are well-established. The discrete semi-norm on $C(\overline{\Psi})$ and the norm on $\Im^{\hbar}$ are both denoted by $|\cdot|_{\hbar}$, which is specified by the expression $[(\cdot, \cdot)^{\hbar}]^{1/2}$. It has been shown that the semi-norm $|\cdot|_{\hbar}$ is equivalent to the norm $|\cdot|_0$, defined as $[(\cdot, \cdot)]^{1/2}$. This equivalence is expressed as:

$$\|\vartheta\|_0^2 \leq |\vartheta|_{\hbar}^2 \leq (d + 2)\|\vartheta\|_0^2 \quad \forall \vartheta \in \Im^{\hbar}, \quad d = 1, 2, 3. \tag{2.3}$$

The Poincaré inequality, assuming h is sufficiently small, can be formulated as follows:

$$((\zeta, \zeta)^{\hbar})^{\frac{1}{2}} = |\zeta|_{\hbar} \leq C_p(|\zeta|_1 + |(\zeta, 1)^{\hbar}|). \tag{2.4}$$

For any $\lambda(u) \in \Im^{\hbar}$, we define that

$$|\lambda^{\hbar}|_{\hbar,\zeta} := (\int_{\Psi} \pi^{\hbar}\{|\lambda(u)^{\hbar}|^{\zeta}\}du)^{\frac{1}{\zeta}} \equiv (\sum_{i=0}^{k} \widehat{M}_{jj}\lambda(u_i)^{\hbar}|^{\zeta})^{\frac{1}{\zeta}} \quad if \quad 0 \leq \zeta < \infty, \tag{2.5}$$

and

$$|\lambda^{\hbar}|_{\hbar,\zeta} := \max_{0 \leq j \leq k} |\lambda(u_j)^{\hbar}| \qquad if \quad \zeta = \infty. \tag{2.6}$$

Next, we review some well-known results regarding the space $\Im^{\hbar}$ under the assumption that $\mathcal{T}^{\hbar}$ constitutes a quasi-uniform partition: For any $\tau \in \mathcal{T}^{\hbar}, \xi \in \Im^{\hbar}, 1 \leq p, q \leq \infty$ and $m, l \in \{0, 1\}$ with $l \leq m$, it holds that

$$\|\xi\|_{m,p,"\tau"} \leq C h_{"\tau"}^{l-m+\ell \min(0, \frac{1}{p}-\frac{1}{q})} \|\xi\|_{l,q,"\tau"}, \tag{2.7}$$

where the abbreviation "τ" means "with" or "without" τ. The inequality above is often termed 'the inverse inequality,' as noted in [15] on pages 75-77. Furthermore, it holds when substituting $\|\cdot\|$ with $|\cdot|$, as documented in [6] on pages 140-142.

For reference, we present the following inverse inequalities, which are derived based on the quasi-uniform condition described in Theorem 3.2.6 of [6]

$$|\xi|_{1,p,"\tau"} \leq C h_{"\tau"}^{-1} |\xi|_{0,p,"\tau"}, \quad 1 \leq p \leq \infty, \tag{2.8}$$

$$|\xi|_{m,p,"\tau"} \leq C h_{"\tau"}^{-\ell(\frac{1}{q}-\frac{1}{p})} |\xi|_{m,q,"\tau"}, \quad 1 \leq q \leq p \leq \infty, \quad m \in \{0, 1\}. \tag{2.9}$$

We additionally require the following interpolation outcomes for every $\xi \in W^{1,s}(\Psi)$, where s belongs to $[2, \infty]$ if $d = 1$, and to $(d, \infty]$ if d is either 2 or 3:

$$|(I - \pi^{\hbar})\xi|_{m,s} \leq C h^{1-m} |\xi|_{1,s}, \quad m \in \{0, 1\}, \tag{2.10}$$

$$\lim_{\hbar \to 0} |(I - \pi^{\hbar})\xi|_{1,s} = 0. \tag{2.11}$$

(see Theorem 1.103 and Corollary 1.110 in [30] respectively). We also recall the following helpful result (see, for example, [8]): for any $\xi_1, \xi_2 \in \Im^{\hbar}$, it holds that

$$|(\xi_1, \xi_2) - (\xi_1, \xi_2)^{\hbar}| \leq C h^{1+m} |\xi_1|_{m,n_1} |\xi_2|_{1,n_2}. \tag{2.12}$$

for $m \in \{0, 1\}$ and $1 \leq n_1, n_2 \leq \infty$ with $\frac{1}{n_1} + \frac{1}{n_2} = 1$. We additionally require the following properties (see [7]):

$$\|(I - \pi^{\hbar})\varsigma\|_0 + h|(I - \pi^{\hbar})\varsigma|_1 \leq C h^2 |\varsigma|_2, \ \text{ for all } \varsigma \in H^2(\Psi), \tag{2.13}$$

$$\|(I - \pi^{\hbar})\varsigma\|_{0,1} \leq C h^2 |\varsigma|_{2,1}, \ \ \forall\ \varsigma \in W^{2,1}(\Psi). \tag{2.14}$$

It is helpful to present the 'inverse Laplacian Green's operator,' denoted by $\mathcal{G}$, which maps $\mathcal{D}_0$ to V_0, such that

$$(\nabla \mathcal{G} v_1, \nabla v_2) = \langle v_1, v_2 \rangle, \qquad \forall\ v_2 \in H^1(\Psi). \tag{2.15}$$

where $\mathcal{D}_0 = \{v \in (H^1(\Psi))' : \langle v, 1 \rangle = 0\}$ and $V_0 = \{v \in H^1(\Psi) : (v, 1) = 0\}$ and $\langle ., . \rangle$ denotes the duality pairing between $(H^1(\Psi))'$ and $H^1(\Psi)$ such that

$$\langle h, v \rangle = (h, v), \quad \forall\ h \in L^2(\Psi) \ \text{ and } \ v \in H^1(\Psi). \tag{2.16}$$

The well-posedness of the operator $\mathcal{G}$ is established by the generalized Lax-Milgram theorem, which also guarantees the existence of a positive constant C such that

$$\|\mathcal{G}_q \sigma\|_{1,q} \leq C \|\sigma\|_{(W^{1,q'}(\Psi))'}, \quad \forall \sigma \in (W^{1,q'}(\Psi))'. \tag{2.17}$$

Furthermore, for any $q \in (1, 2]$, the following holds:

$$\|\chi\|_{0,q} \leq C h^{-1} \|\mathcal{G}_q \chi\|_{1,q}, \quad \forall \chi \in \Im^{\hbar}. \tag{2.18}$$

It is also helpful to state the following result: For $1 \leq r < \infty$, we have that:

$$|\varsigma|_{2,r} \leq \Big(\int_{\Re} \sum_{k,m}^{k} \Big| \frac{\partial^2 \varsigma}{\partial x_k x_m} \Big|^r d\mathbf{x} \Big)^{\frac{1}{r}} \leq 2^{\frac{1}{r}} |\varsigma|_{2,r}, \ \text{ for all } \varsigma \in W^{2,r}(\Psi). \tag{2.19}$$

The inverse inequalities are also presented here: For all $\varsigma \in \Im^{\hbar}$, as seen in [6], it holds that:

$$|\varsigma|_{1,r,"\tau"} \leq Ch_{"\tau"}^{-1}|\varsigma|_{0,r,"\tau"}, \quad 1 \leq r \leq \infty, \tag{2.20}$$

$$\|\varsigma\|_{0,r_2,"\tau"} \leq Ch_{"\tau"}^{-d(\frac{1}{r_1}-\frac{1}{r_2})}\|\varsigma\|_{0,r_1,"\tau"}, \quad 1 \leq r_1 \leq r_2 \leq \infty, \tag{2.21}$$

$$|\varsigma|_{1,r_2,"\tau"} \leq Ch_{"\tau"}^{-d(\frac{1}{r_1}-\frac{1}{r_2})}|\varsigma|_{1,r_1,"\tau"}, \quad 1 \leq r_1 \leq r_2 \leq \infty. \tag{2.22}$$

3 A semi-discrete approximation

We present the subsequent SDA for the system (1.4)-(1.7)
(Θ^h) Find $\{\xi^{\hbar}, \gamma^{\hbar}\} \in \Im^{\hbar} \times \Im^{\hbar}$ such that for a.e. $t \in (0,T)$

$$(\frac{\partial \xi^{\hbar}}{\partial t}, \mu^{\hbar})^{\hbar} + (\nabla\gamma^{\hbar}, \nabla\mu^{\hbar}) + ((\gamma^{\hbar})^3, \mu^{\hbar})^{\hbar} = 0, \qquad \forall \mu^{\hbar} \in \Im^{\hbar}, \tag{3.1}$$

$$(\frac{\partial \gamma^{\hbar}}{\partial t}, \mu^{\hbar})^{\hbar} + (\gamma^{\hbar}, \mu^{\hbar})^{\hbar} = (\xi^{\hbar}, \mu^{\hbar})^{\hbar}, \qquad \forall\ \mu^{\hbar} \in \Im^{\hbar}, \tag{3.2}$$

$$\gamma^{\hbar}(.,0) = \mathbb{P}^{\hbar}\gamma_1(.) \qquad \xi^{\hbar}(\cdot,0) = \mathbb{P}^{\hbar}\gamma_1^0 + \mathbb{P}^{\hbar}\gamma_2^0. \tag{3.3}$$

3.1 Global existence

For a variety of motives it is essential to determine boundaries on solution spaces while solving partial differential equations (PDEs) numerically. Fluid dynamics, heat transport, electromagnetic fields, and quantum physics are just a few of the many natural and artificial systems that PDEs may simulate. There are several advantages to establishing suitable boundaries on the solution spaces in order to comprehend and successfully approximate complex systems. Researchers provide a framework for reliable, effective, and precise numerical solutions by putting theoretical or empirical constraints on solution spaces. This method improves the overall applicability and dependability of numerical PDE solvers across several disciplines in addition to helping with problem-specific analysis.

Theorem 3.1. *Consider an open, bounded, convex domain $\Psi \subset \mathbb{R}^d$ (with $d \leq 3$). Let $\gamma^0 \in H^1(\Psi)$. Then, the system (3.1)-(3.3) has a solution $\gamma^{\hbar}, \xi^{\hbar}$ that satisfies:*

$$\gamma^{\hbar} \in L^2(0,T;H^1(\Psi)) \cap L^2(\Psi_T) \cap L^4(\Psi_T) \cap L^{\infty}(0,T;L^2(\Psi)), \tag{3.4}$$

$$\xi^{\hbar} \in L^2(\Psi_T), \tag{3.5}$$

$$\frac{\partial \gamma^{\hbar}}{\partial t} \in L^2(\Psi_T). \tag{3.6}$$

Proof: Next, we examine the following free energy expression in the form:

$$E(\gamma^{\hbar}, \xi^{\hbar}) = \|\xi^{\hbar}\|_0^2 + |\gamma^{\hbar}|_1^2 + \frac{1}{2}\|\gamma^{\hbar}\|_4^4. \tag{3.7}$$

By differentiating $E(\gamma^{\hbar}, \xi^{\hbar})$ with respect to t, we obtain that

$$\frac{\partial}{\partial t}E(\gamma^{\hbar}, \xi^{\hbar}) = 2(\xi^{\hbar}, \frac{\partial \xi^{\hbar}}{\partial t})^{\hbar} + 2(\nabla\gamma^{\hbar}, \nabla\frac{\partial \gamma^{\hbar}}{\partial t}) + 2((\gamma^{\hbar})^3, \frac{\partial \gamma^{\hbar}}{\partial t})^{\hbar}. \tag{3.8}$$

Substituting $\mu^{\hbar} = \frac{\partial \gamma^{\hbar}}{\partial t}$ into (3.1), we obtain

$$(\frac{\partial \xi^{\hbar}}{\partial t}, \frac{\partial \gamma^{\hbar}}{\partial t})^{\hbar} + (\nabla\gamma^{\hbar}, \nabla\frac{\partial \gamma^{\hbar}}{\partial t}) + ((\gamma^{\hbar})^3, \frac{\partial \gamma^{\hbar}}{\partial t})^{\hbar} = 0, \tag{3.9}$$

$$(\nabla\gamma^{\hbar}, \nabla\frac{\partial\gamma^{\hbar}}{\partial t}) + ((\gamma^{\hbar})^3, \frac{\partial\gamma^{\hbar}}{\partial t})^{\hbar} = -(\frac{\partial\xi^{\hbar}}{\partial t}, \frac{\partial\gamma^{\hbar}}{\partial t})^{\hbar}. \tag{3.10}$$

By inserting (3.10) into (3.8), we get that

$$\frac{\partial}{\partial t}E(\gamma^{\hbar}, \xi^{\hbar}) = 2(\xi^{\hbar}, \frac{\partial\xi^{\hbar}}{\partial t})^{\hbar} - 2(\frac{\partial\xi^{\hbar}}{\partial t}, \frac{\partial\gamma^{\hbar}}{\partial t})^{\hbar}, \tag{3.11}$$

Substituting $\mu^{\hbar} = \frac{\partial\xi^{\hbar}}{\partial t}$ into (3.2), it follows that

$$(\frac{\partial\gamma^{\hbar}}{\partial t}, \frac{\partial\xi^{\hbar}}{\partial t})^{\hbar} = (\xi^{\hbar}, \frac{\partial\xi^{\hbar}}{\partial t})^{\hbar} - (\gamma^{\hbar}, \frac{\partial\xi^{\hbar}}{\partial t})^{\hbar}, \tag{3.12}$$

Next, by substituting (3.12) into (3.11), we arrive at

$$\frac{\partial}{\partial t}E(\gamma^{\hbar}, \xi^{\hbar}) = 2(\gamma^{\hbar}, \frac{\partial\xi^{\hbar}}{\partial t})^{\hbar}. \tag{3.13}$$

By selecting $\mu^{\hbar} = \gamma^{\hbar}$ in (3.1), we conclude that

$$(\frac{\partial\xi^{\hbar}}{\partial t}, \gamma^{\hbar})^{\hbar} = -\|\nabla\gamma^{\hbar}\|_0^2 - \|\gamma^{\hbar}\|_4^4. \tag{3.14}$$

By substituting (3.14) into (3.13), we get

$$\frac{\partial}{\partial t}E(\gamma^{\hbar}, \xi^{\hbar}) = -2\|\nabla\gamma^{\hbar}\|_0^2 - 2\|\gamma^{\hbar}\|_4^4 \leq 0. \tag{3.15}$$

Thus, E is a Lyapunov functional. By integrating equation (3.15) from 0 to t and considering equation (3.3), it can be deduced that

$$E(\gamma^{\hbar}(t), \xi^{\hbar}(t)) \leq E(\mathbb{P}^{\hbar}\gamma^0, \mathbb{P}^{\hbar}\xi^0). \tag{3.16}$$

Given equations (2.1) and (2.3), along with the assumption that $\gamma^0, \xi^0 \in H^1(\Psi)$, it follows that

$$E(\mathbb{P}^{\hbar}\gamma^0, \mathbb{P}^{\hbar}\xi^0) \leq \int_{\Psi}[\|\mathbb{P}^{\hbar}\xi^0\|_0^2 + |\mathbb{P}^{\hbar}\nabla\gamma^0|^2 + \frac{1}{2}\|\mathbb{P}^{\hbar}\gamma^0\|_4^4]d\mathbf{x}$$

$$\leq \|\xi^0\|_{\hbar}^2 + |\gamma^0|_1^2 + \frac{1}{2}\|\gamma^0\|_{\hbar}^4 \leq C. \tag{3.17}$$

From the above results and (3.16), it can be concluded that

$$E(\gamma^{\hbar}(t), \xi^{\hbar}(t)) \leq C. \tag{3.18}$$

Next, by replacing equation (3.7) into (3.18), it follows that

$$\|\xi^{\hbar}\|_0^2 + |\gamma^{\hbar}|_1^2 + \frac{1}{2}\|\gamma^{\hbar}\|_4^4 \leq C, \tag{3.19}$$

which leads to

$$\|\xi^{\hbar}\|_{L^2(\Psi_T)} \leq C, \qquad \|\gamma^{\hbar}\|_{L^2(0,T;H^1(\Psi))} \leq C, \qquad \|\gamma^{\hbar}\|_{L^4(\Psi_T)} \leq C. \tag{3.20}$$

Now, by substituting $\mu^{\hbar} = \gamma^{\hbar}$ into equation (3.2), it can be concluded that

$$\frac{d}{2dt}\|\gamma^{\hbar}\|_0^2 + \|\gamma^{\hbar}\|_0^2 \leq (\gamma^{\hbar}, \xi^{\hbar})^{\hbar}. \tag{3.21}$$

By applying Young's inequality, it can be stated that

$$\frac{d}{2dt}\|\gamma^{\hbar}\|_0^2 + \frac{1}{2}\|\gamma^{\hbar}\|_0^2 \leq \frac{1}{2}\|\xi^{\hbar}\|_0^2. \tag{3.22}$$

Upon integrating both sides of equation (3.22) from 0 to t, the outcome is

$$\|\gamma^{\hbar}(T)\|_0^2 + \int_0^T \|\gamma^{\hbar}\|_0^2 dt \leq \int_0^T \|\xi^{\hbar}\|_0^2 + \|\gamma^{\hbar}(0)\|_0^2. \tag{3.23}$$

Based on equations (3.20) and (3.23), and under the assumption that $\gamma_1^0 \in H^1(\Psi)$, we find that

$$\|\gamma^{\hbar}\|_{L^\infty(0,T;L^2(\Psi))} \leq C, \qquad \|\gamma^{\hbar}\|_{L^2(\Psi_T)} \leq C. \tag{3.24}$$

By selecting $\mu^{\hbar} = \frac{\partial \gamma^{\hbar}}{\partial t}$ in equation (3.2), it follows that

$$\|\frac{\partial \gamma^{\hbar}}{\partial t}\|_0^2 + \frac{d}{2dt}\|\gamma^{\hbar}\|_0^2 = (\xi^{\hbar}, \frac{\partial \gamma^{\hbar}}{\partial t})^{\hbar}. \tag{3.25}$$

By utilizing Young's inequality, it can be represented that

$$\frac{1}{2}\|\frac{\partial \gamma^{\hbar}}{\partial t}\|_0^2 + \frac{d}{2dt}\|\gamma^{\hbar}\|_0^2 \leq \frac{1}{2}\|\xi^{\hbar}\|_0^2. \tag{3.26}$$

By integrating equation (3.26) over the interval (0,T) and applying equation (3.20), it can be deduced that

$$\int_0^T \|\frac{\partial \gamma^{\hbar}}{\partial t}\|_0^2 dt + \|\gamma^{\hbar}(T)\|_0^2 \leq \int_0^T \|\xi^{\hbar}\|_0^2 dt + \|\gamma^{\hbar}(0)\|_0^2. \tag{3.27}$$

Based on equation (3.28) and under the assumption that γ_1^0 belongs to $H^1(\Psi)$, it follows that

$$\|\frac{\partial \gamma^{\hbar}}{\partial t}\|_{L^2(\Psi_T)} \leq C. \tag{3.28}$$

□

4 A fully-discrete approximation

Let L be a positive integer, and define the time step as $\Delta t := \frac{T}{L}$. We now consider the following FDA for the system described by equations (1.4)-(1.7):
$(\Theta^{\hbar,\Delta t})$ Find $\Xi^{\ell}(.,t), \Gamma^{\ell}(.,t) \in \Im^{\hbar} \times \Im^{\hbar}$ such that $\forall\ \Sigma \in \Im^{\hbar}$

$$\Big(\frac{\Xi^{\ell} - \Xi^{\ell-1}}{\Delta t}, \Sigma\Big)^{\hbar} + (\nabla\Gamma^{\ell}, \nabla\Sigma) + ((\Gamma^{\ell})^3, \Sigma)^{\hbar} = 0 \qquad \forall \Sigma \in \Im^{\hbar}, \tag{4.1}$$

$$\Big(\frac{\Gamma^{\ell} - \Gamma^{\ell-1}}{\Delta t}, \Sigma\Big)^{\hbar} + (\Gamma^{\ell}, \Sigma)^{\hbar} = (\Xi^{\ell}, \Sigma)^{\hbar} \qquad \forall \Sigma \in \Im^{\hbar}, \tag{4.2}$$

$$\Gamma^0 = P^{\hbar}\gamma_1^0, \qquad \Xi^0 = P^{\hbar}\gamma_1^0 + P^{\hbar}\gamma_2^0 = P^{\hbar}\xi^0. \tag{4.3}$$

For future reference, it is important to keep the following points in mind:

$$2a(a-b) = a^2 + (a-b)^2 - b^2, \ \ \forall a, b \in \mathbb{R}. \tag{4.4}$$

Theorem 4.1. *Let Ψ and $\mathcal{T}^{\hbar}$ be such that assumption (A) is satisfied, and let $\gamma^0 \in H^1(\Psi) \cap L^4(\Psi)$ and $\xi^0 \in L^2(\Psi)$. Then, for every $\Delta t > 0$, there exists a solution $\{\Xi^{\ell}, \Gamma^{\ell}\}_{\ell=1}^{L}$ to $(\Theta^{\hbar,\Delta t})$. The following stability bounds are then valid:*

$$\max_{\jmath=1,\ldots,L}[|\Gamma^{\jmath}|_{\hbar}^2] + \sum_{\ell=1}^{\jmath}[\Delta t|\Xi^{\ell} - \Xi^{\ell-1}|_{\hbar}^2 + \Delta t\|\nabla(\Gamma^{\ell} - \Gamma^{\ell-1})\|_0^2 + \ |\Gamma^{\ell} - \Gamma^{\ell-1}|_{h}^2] + \sum_{\ell=1}^{\jmath}\Delta t[|\Gamma^{\ell}|_1^2 + |\Gamma^{\ell}|_{h,4}^4 + \frac{1}{2}|\Xi^{\ell}|_{\hbar}^2]$$

$$\leq C^2\Delta t|\Psi|. \tag{4.5}$$

Proof: By selecting $\Sigma = \Gamma^{\ell} - \Gamma^{\ell-1}$ in equation (4.1) and $\Sigma = \Xi^{\ell} - \Xi^{\ell-1}$ in equation (4.2) and $\Sigma = \Gamma^{\ell}$ in equation (4.2), we derive the following results:

$$\frac{1}{\Delta t}(\Xi^{\ell} - \Xi^{\ell-1}, \Gamma^{\ell} - \Gamma^{\ell-1})^{\hbar} + (\nabla\Gamma^{\ell}, \nabla(\Gamma^{\ell} - \Gamma^{\ell-1})) + ((\Gamma^{\ell})^3, \Gamma^{\ell} - \Gamma^{\ell-1})^{\hbar} = 0, \tag{4.6}$$

$$\frac{1}{\Delta t}(\Gamma^{\ell} - \Gamma^{\ell-1}, \Xi^{\ell} - \Xi^{\ell-1})^{\hbar} + (\Gamma^{\ell}, \Xi^{\ell} - \Xi^{\ell-1})^{\hbar} = (\Xi^{\ell}, \Xi^{\ell} - \Xi^{\ell-1})^{\hbar}, \tag{4.7}$$

$$\frac{1}{\Delta t}(\Gamma^{\ell} - \Gamma^{\ell-1}, \Gamma^{\ell})^{\hbar} + (\Gamma^{\ell}, \Gamma^{\ell})^{\hbar} = (\Xi^{\ell}, \Gamma^{\ell})^{\hbar}, \tag{4.8}$$

From equations (4.6) and (4.7), it follows that:

$$\frac{1}{\Delta t}(\Gamma^{\ell} - \Gamma^{\ell-1}, \Gamma^{\ell})^{\hbar} + (\nabla\Gamma^{\ell}, \nabla(\Gamma^{\ell} - \Gamma^{\ell-1})) + ((\Gamma^{\ell})^3, \Gamma^{\ell} - \Gamma^{\ell-1})^{\hbar} + (\Xi^{\ell}, \Xi^{\ell} - \Xi^{\ell-1})^{\hbar} + (\Gamma^{\ell}, \Gamma^{\ell})^{\hbar}$$
$$= (\Gamma^{\ell}, \Xi^{\ell} - \Xi^{\ell-1})^{\hbar} + (\Xi^{\ell}, \Gamma^{\ell})^{\hbar}. \tag{4.9}$$

Applying Taylor's theorem and Young's inequality (2.3) to equation (4), we obtain the following:

$$\begin{aligned}\frac{1}{2\Delta t}|\Gamma^{\ell}|_{\hbar}^2 + \frac{1}{2\Delta t}|\Gamma^{\ell} - \Gamma^{\ell-1}|_{\hbar}^2 - \frac{1}{2\Delta t}|\Gamma^{\ell-1}|_{\hbar}^2 + \frac{1}{2}\|\nabla\Gamma^{\ell}\|_0^2 + \frac{1}{2}\|\nabla(\Gamma^{\ell} - \Gamma^{\ell-1})\|_0^2 - \frac{1}{2}\|\nabla\Gamma^{\ell-1}\|_0^2 + \frac{1}{3}|\Gamma^{\ell}|_{\hbar,4}^4 - \frac{1}{3}|\Gamma^{\ell-1}|_{\hbar,4}^4 \\ + \frac{1}{2}|\Xi^{\ell}|_{\hbar}^2 + \frac{1}{2}|\Xi^{\ell} - \Xi^{\ell-1}|_{\hbar}^2 - \frac{1}{2}|\Xi^{\ell-1}|_{\hbar}^2 + |\Gamma^{\ell}|_{\hbar}^2 \\ \leq 2|\Gamma^{\ell}|_{\hbar}^2 + \frac{1}{4}|\Xi^{\ell} - \Xi^{\ell-1}|_{\hbar}^2 + \frac{1}{4}|\Xi^{\ell}|_{\hbar}^2 \\ \leq C^2|\Psi| + \frac{1}{6}|\Gamma^{\ell}|_{\hbar}^4 + \frac{1}{4}|\Xi^{\ell} - \Xi^{\ell-1}|_{\hbar}^2 + \frac{1}{4}|\Xi^{\ell}|_{\hbar}^2.\end{aligned} \tag{4.10}$$

Thus, it follows that

$$\begin{aligned}\frac{1}{2\Delta t}|\Gamma^{\ell}|_{\hbar}^2 + \frac{1}{2\Delta t}|\Gamma^{\ell} - \Gamma^{\ell-1}|_{\hbar}^2 + \frac{1}{2}\|\nabla\Gamma^{\ell}\|_0^2 + \frac{1}{2}\|\nabla(\Gamma^{\ell} - \Gamma^{\ell-1})\|_0^2 + \frac{1}{2}|\Gamma^{\ell}|_{\hbar,4}^4 + \frac{1}{4}|\Xi^{\ell}|_{\hbar}^2 + \frac{3}{4}|\Xi^{\ell} - \Xi^{\ell-1}|_{\hbar}^2 \\ \leq C^2|\Psi| + \frac{1}{2}\|\nabla\Gamma^{\ell-1}\|_0^2 + \frac{1}{3}|\Gamma^{\ell-1}|_{\hbar,4}^4 + \frac{1}{2}|\Xi^{\ell-1}|_{\hbar}^2 + \frac{1}{2\Delta t}|\Gamma^{\ell-1}|_{\hbar}^2.\end{aligned} \tag{4.11}$$

By adding the equation above for $\ell = 1, \ldots, \jmath$ with $\jmath \leq L$, multiplying the outcome by Δt, and applying the assumptions regarding the initial conditions, it follows that

$$\begin{aligned}\max_{\jmath=1,\ldots,L}[|\Gamma^{\jmath}|_{\hbar}^2] + \sum_{\ell=1}^{\jmath}[\Delta t|\Xi^{\ell} - \Xi^{\ell-1}|_{\hbar}^2 + \Delta t\|\nabla(\Gamma^{\ell} - \Gamma^{\ell-1})\|_0^2 + |\Gamma^{\ell} - \Gamma^{\ell-1}|_{\hbar}^2] + \sum_{\ell=1}^{\jmath}\Delta t[|\Gamma^{\ell}|_1^2 + |\Gamma^{\ell}|_{\hbar,4}^4 + \frac{1}{2}|\Xi^{\ell}|_{\hbar}^2] \\ \leq C^2\Delta t|\Psi| + |\Gamma^0|_{\hbar}^2 + |\Gamma^0|_1^2 + |\Gamma^0|_{\hbar,4}^4 + |\Xi^0|_{\hbar}^2 \leq C^2\Delta t|\Psi|.\end{aligned} \tag{4.12}$$

□

4.1 Existence of fully-discrete approximation

To confirm the accuracy and suitability of numerical techniques in capturing the behaviour of intricate physical systems, it is crucial to investigate the existence of FDA for solving PDEs. FDA is frequently employed to approximate PDE approximations, particularly in disciplines like economics, physics, and engineering. The precision, consistency, and interpretability of these answers are supported by the presence of a FEA. Any meaningful numerical solution requires that the problem be well-posed, which means that it has a solution, and that solution must be distinct and continuously dependent on the input data. The first of these requirements is satisfied by the presence of a

FDA, which confirms that the selected finite-dimensional function space has an approximate solution. Without this guarantee, calculations can provide inaccurate or non-physical outcomes.

Our goal while researching FDA is to make sure that the numerical solution converges to the actual solution of the PDE as the mesh is refined, that is, as the elements grow smaller or the function space gets richer. The availability of a FDA helps confirm that as the resolution grows, the technique will approach the correct solution, which is important for both theoretical analysis and practical implementation. To sum up, confirming that finite element techniques yield dependable, stable, and convergent solutions requires first examining the presence of FDA. This theoretical foundation encourages the development of more advanced techniques that can manage complicated and high-dimensional PDEs in addition to boosting confidence in the utilise of FDA for a variety of applications.

Employing a methodology similar to that outlined in [18, 19, 20, 21, 26, 24, 27, 1, 25, 2, 3, 22, 23], we define the functions as follows: $A_\Xi : \Im^\hbar \times \Im^\hbar \to \Im^\hbar$ and $A_\Gamma : \Im^\hbar \times \Im^\hbar \to \Im^\hbar$, such that for every $\Sigma \in \Im^\hbar$:

$$(A_\Xi(\Xi,\Gamma),\ \Sigma)^\hbar = (\Xi - \Xi^{\ell-1},\ \Sigma)^\hbar + \Delta t(\nabla\Gamma,\ \nabla\Sigma) + \Delta t(\Gamma^3,\ \Sigma)^\hbar, \tag{4.13}$$

$$(A_\Gamma(\Xi,\Gamma),\ \Sigma)^\hbar = (\Gamma - \Gamma^{\ell-1},\ \Sigma)^\hbar + \Delta t(\Gamma,\ \Sigma)^\hbar - \Delta t(\Xi,\ \Sigma)^\hbar. \tag{4.14}$$

respectively. We begin by noting that the continuous piecewise linear functions A_Ξ and A_Γ can be uniquely determined from their values at the nodal points $N^\hbar$. This uniqueness is clear when we set $\Sigma \equiv \kappa_j$, where $j = 0, \ldots, J$, in (4.13) and (4.14). This leads to the derivation of solvable systems of square matrices as follows:

$$MA_\Xi(\Xi,\Gamma) = S_1, \qquad MA_\Gamma(\Xi,\Gamma) = S_2.$$

Here, the matrix M represents the lumped mass matrix, while S_1 and S_2 are vectors expressed in terms of the nodal values of Ξ, Γ, $\Xi^{\ell-1}$, and $\Gamma^{\ell-1}$. As a result, the functions A_Ξ and A_Γ are properly defined.

By examining (4.13) and (4.14), the problem $(\Theta^{\hbar,\Delta t})$ can be restated as:
For given $\{\Xi^0, \Gamma^0\} \in \Im^\hbar \times \Im^\hbar$, find $\{\Xi^\ell, \Gamma^\ell\} \in \Im^\hbar \times \Im^\hbar$, $\ell \geq 1$, such that

$$A_\Xi(\Xi,\Gamma) = 0, \qquad A_\Gamma(\Xi,\Gamma) = 0. \tag{4.15}$$

Lemma 4.2. *For any $\beta > 0$, the functions $A_\Xi : [\Im^\hbar]^2_\beta \to \Im^\hbar$ and $A_\Gamma : [\Im^\hbar]^2_\beta \to \Im^\hbar$ demonstrate continuity in the following way:*

$$[\Im^\hbar]^2_\beta = \left\{ \{\Upsilon_1, \Upsilon_2\} \in \Im^\hbar \times \Im^\hbar : |\Upsilon_1|^2_\hbar + |\Upsilon_2|^2_\hbar \leq \beta^2 \right\}.$$

Proof: Let Ξ_1, Γ_1 and $\Xi_2, \Gamma_2 \in [\Im^\hbar]^2$. From (4.13), for every $\Sigma \in \Im^\hbar$, it follows that:

$$(A_\Gamma(\Xi_1,\Gamma_1) - A_\Gamma(\Xi_2,\Gamma_2),\ \Sigma)^\hbar = (\Xi_1 - \Xi_2,\ \Sigma)^\hbar + \Delta t(\nabla\Gamma_1 - \nabla\Gamma_2,\ \nabla\Sigma) + \Delta t((\Gamma_1)^3 - (\Gamma_2)^3,\ \Sigma)^\hbar. \tag{4.16}$$

By selecting $\Sigma = A_\Gamma(\Xi_1,\Gamma_1) - A_\Gamma(\Xi_2,\Gamma_2)$ in (4.16), and applying the Cauchy-Schwarz inequality, along with (2.20) and (2.3), it follows that:

$$\begin{aligned}
|A_\Gamma(\Xi_1,\Gamma_1) - A_\Gamma(\Xi_2,\Gamma_2)|^2_\hbar &= (\Xi_1 - \Xi_2,\ A_\Gamma(\Xi_1,\Gamma_1) - A_\Gamma(\Xi_2,\Gamma_2))^\hbar \\
&+\Delta t(\nabla\Gamma_1 - \nabla\Gamma_2,\ \nabla(A_\Gamma(\Xi_1,\Gamma_1) - A_\Gamma(\Xi_2,\Gamma_2))) + \Delta t((\Gamma_1)^3 - (\Gamma_2)^3,\ A_\Gamma(\Xi_1,\Gamma_1) - A_\Gamma(\Xi_2,\Gamma_2))^\hbar \\
&\leq |\Xi_1 - \Xi_2|_\hbar |A_\Gamma(\Xi_1,\Gamma_1) - A_\Gamma(\Xi_2,\Gamma_2|_\hbar + \Delta t|\Gamma_1 - \Gamma_2|_1 |A_\Gamma(\Xi_1,\Gamma_1) - A_\Gamma(\Xi_2,\Gamma_2)|_1 \\
&+\Delta t|(\Gamma_1)^3 - (\Gamma_2)^3|_\hbar |A_\Gamma(\Xi_1,\Gamma_1) - A_\Xi(\Xi_2,\Gamma_2)|_\hbar \\
&\leq |\Xi_1 - \Xi_2|_\hbar |A_\Gamma(\Xi_1,\Gamma_1) - A_\Gamma(\Xi_2,\Gamma_2|_\hbar + \Delta t C h^{-1} |\Gamma_1 - \Gamma_2|_\hbar |A_\Gamma(\Xi_1,\Gamma_1) - A_\Gamma(\Xi_2,\Gamma_2)|_\hbar \\
&+\Delta t|(\Gamma_1)^3 - (\Gamma_2)^3|_\hbar |A_\Gamma(\Xi_1,\Gamma_1) - A_\Gamma(\Xi_2,\Gamma_2)|_\hbar.
\end{aligned} \tag{4.17}$$

The Cauchy-Schwarz inequality implies that

$$\Delta t|\Gamma_1^3 - \Gamma_2^3|_\hbar \leq C\Delta t(|\Gamma_1|^2_{\hbar,\infty} + |\Gamma_2|^2_{\hbar,\infty})|\Gamma_1 - \Gamma_2|_\hbar \leq C\Delta t|\Gamma_1 - \Gamma_2|_\hbar. \tag{4.18}$$

From the above results and (4.18), it follows that:

$$|A_\Gamma(\Xi_1,\Gamma_1)-A_\Gamma(\Xi_2,\Gamma_2)|_\hbar^2 \le C(h^{-1},\Delta t)(|\Xi_1-\Xi_2|_\hbar+|\Gamma_1-\Gamma_2|_\hbar). \tag{4.19}$$

From (4.14), we can deduce, for every $\Sigma \in \Im^\hbar$, that

$$(A_\Xi(\Xi_1,\Gamma_1)-A_\Xi(\Xi_2,\Gamma_2),\ \Sigma)^\hbar = (\Gamma_1-\Gamma_2,\ \Sigma)^\hbar + \Delta t(\Gamma_1-\Gamma_2,\ \Sigma)^\hbar - \Delta t(\Xi_1-\Xi_2,\ \Sigma)^\hbar. \tag{4.20}$$

Let $\Sigma = A_\Xi(\Xi_1,\Gamma_1)-A_\Xi(\Xi_2,\Gamma_2)$, and by applying the Cauchy-Schwarz inequality, it follows that

$$|A_\Xi(\Xi_1,\Gamma_1)-A_\Xi(\Xi_2,\Gamma_2)|_\hbar^2 \le |\Gamma_1-\Gamma_2|_\hbar |A_\Xi(\Xi_1,\Gamma_1)-A_\Xi(\Xi_2,\Gamma_2)|_\hbar$$

$$+\Delta t|\Gamma_1-\Gamma_2|_\hbar |A_\Xi(\Xi_1,\Gamma_1)-A_\Xi(\Xi_2,\Gamma_2)|_\hbar + \Delta t|\Xi_1-\Xi_2|_\hbar |A_\Xi(\Xi_1,\Gamma_1)-A_\Xi(\Xi_2,\Gamma_2)|_\hbar.$$

By utilizing equation (2.3), it can be concluded that

$$|A_\Xi(\Xi_1,\Gamma_1)-A_\Xi(\Xi_2,\Gamma_2)|_\hbar \le |\Gamma_1-\Gamma_2|_\hbar + \Delta t|\Gamma_1-\Gamma_2|_\hbar + \Delta t|\Xi_1-\Xi_2|_\hbar.$$

Therefore, it follows that

$$|A_\Xi(\Xi_1,\Gamma_1)-A_\Xi(\Xi_2,\Gamma_2)|_\hbar \le C\Delta t(|\Gamma_1-\Gamma_2|_\hbar+|\Xi_1-\Xi_2|_\hbar). \tag{4.21}$$

The results in (4.19) and (4.21) show that A_Ξ and A_Γ are, respectively, Lipschitz continuous. □

Theorem 4.3. *Assume that $\Gamma^{\ell-1}$ and $\Xi^{\ell-1} \in \Im^\hbar$ constitute a solution to the $(\ell-1)$-th step of $(\Theta^{\hbar,\Delta t})$ for some $\ell = 1,2,\dots,L$. Then, for every $h>0$, there exists a solution $\{\Xi,\Gamma\} \in [\Im^\hbar]^2_\Psi$ to the ℓ-th step of $(\Theta^{\hbar,\Delta t})$.*

Proof: Assume $\beta > 0$ and consider the case where there is no pair $\{\Xi,\Gamma\} \in \Im^\hbar \times \Im^\hbar$ such that $A_\Xi(\Xi,\Gamma) = A_\Gamma(\Xi,\Gamma) = 0$. Given the continuity of the functions $A_\Xi(\Xi,\Gamma)$ and $A_\Gamma(\Xi,\Gamma)$ on $[\Im^\hbar]^2_\beta$, we can define the continuous function $\mathcal{G} : [\Im^\hbar]^2_\beta \to [\Im^\hbar]^2_\beta$ as

$$\mathcal{G}(\Xi,\Gamma) = (\mathcal{G}_\Xi(\Xi,\Gamma),\mathcal{G}_\Gamma(\Xi,\Gamma)),$$

Here, the functions $\mathcal{G}_\Xi(\Xi,\Gamma)$ and $\mathcal{G}_\Gamma(\Xi,\Gamma)$ are given by:

$$\begin{aligned} \mathcal{G}_\Xi(\Xi,\Gamma) &:= \frac{-\beta A_\Xi(\Xi,\Gamma)}{|(A_\Xi(\Xi,\Gamma),A_\Gamma(\Xi,\Gamma))|_{\Im^\hbar\times\Im^\hbar}}, \\ \mathcal{G}_\Gamma(\Xi,\Gamma) &:= \frac{-\beta A_\Gamma(\Xi,\Gamma)}{|(A_\Xi(\Xi,\Gamma),A_\Gamma(\Xi,\Gamma))|_{\Im^\hbar\times\Im^\hbar}}. \end{aligned} \tag{4.22}$$

Where $|(.,.)|_{[\Im^\hbar]^2_\beta}$ denotes the standard norm on $[\Im^\hbar]^2_\beta$, defined by

$$|(\Upsilon_1,\Upsilon_2)|_{\Im^\hbar\times\Im^\hbar} = (\sum_{i=1}^{2}|\Upsilon_i|_\hbar^2)^{\frac{1}{2}}.$$

The continuity of the function $\mathcal{G}$ follows from the continuity of A_Ξ and A_Γ, as shown in Lemma 4.2. Since $[\Im^\hbar]^2_\beta$ is a convex and compact subset of $\Im^\hbar \times \Im^\hbar$, Schauder's fixed-point theorem guarantees the existence of $\Xi,\Gamma \in [\Im^\hbar]^2_\beta$ that are fixed points of $\mathcal{G}$, of the form

$$\mathcal{G}(\Xi,\Gamma) = (\mathcal{G}_\Xi(\Xi,\Gamma),\mathcal{G}_\Gamma(\Xi,\Gamma)) = (\Xi,\Gamma).$$

From (4.22), we also observe that the fixed point $\{\Xi,\Gamma\}$ satisfies the condition that

$$|\Xi|_\hbar^2 + |\Gamma|_\hbar^2 = |\mathcal{G}_\Xi(\Xi,\Gamma)|_\hbar^2 + |\mathcal{G}_\Gamma(\Xi,\Gamma)|_\hbar^2 = \beta^2. \tag{4.23}$$

By selecting $\Sigma \equiv \Gamma - \Gamma^{\ell-1}$ in (4.13) and $\Sigma \equiv \Xi - \Xi^{\ell-1}$ in (4.14), we can conclude that

$$\big(A_\Gamma(\Xi,\Gamma),\Gamma-\Gamma^{\ell-1}\big)^\hbar = \big(\Xi-\Xi^{\ell-1},\Gamma-\Gamma^{\ell-1}\big)^\hbar + \Delta t\big(\nabla\Gamma,\ \nabla(\Gamma-\Gamma^{\ell-1})\big) + \Delta t\big(\Gamma^3,\Gamma-\Gamma^{\ell-1}\big)^\hbar, \tag{4.24}$$

$$\big(A_\Xi(\Xi,\Gamma),\Xi-\Xi^{\ell-1}\big)^\hbar = (\Gamma-\Gamma^{\ell-1},\ \Xi-\Xi^{\ell-1})^\hbar + \Delta t(\Gamma,\ \Xi-\Xi^{\ell-1})^\hbar - \Delta t(\Xi,\ \Xi-\Xi^{\ell-1})^\hbar. \tag{4.25}$$

It follows from (4.4) that

$$(\nabla\Gamma,\ \nabla(\Gamma-\Gamma^{\ell-1}))^\hbar \geq \frac{1}{2}\big(|\nabla\Gamma|_\hbar^2 - |\nabla\Gamma^{\ell-1}|_\hbar^2\big), \tag{4.26}$$

$$(\Xi,\ \Xi-\Xi^{\ell-1})^\hbar = \frac{1}{2}(|\Xi|_\hbar^2 + |\Xi-\Xi^{\ell-1}|_\hbar^2 - |\Xi^{\ell-1}|_\hbar^2), \tag{4.27}$$

$$(\Gamma^3,\Gamma-\Gamma^{\ell-1})^\hbar \geq \frac{1}{3}\big(|\Gamma|_{\hbar,4}^4 - |\Gamma^{\ell-1}|_{\hbar,4}^4\big). \tag{4.28}$$

By combining (4.24) and (4.25), along with observing (4.26), (4.27), and (4.28), and applying Young's inequality, it follows that for sufficiently large β

$$\begin{aligned}
&\big(A_\Gamma(\Xi,\Gamma),\Gamma-\Gamma^{\ell-1}\big)^\hbar - \big(A_\Xi(\Xi,\Gamma),\Xi-\Xi^{\ell-1}\big)^\hbar \\
&\geq \frac{\Delta t}{2}\big(|\nabla\Gamma|_\hbar^2 - |\nabla\Gamma^{\ell-1}|_\hbar^2\big) + \frac{\Delta t}{2}(|\Xi|_\hbar^2 + |\Xi-\Xi^{\ell-1}|_\hbar^2 - |\Xi^{\ell-1}|_\hbar^2) + \frac{\Delta t}{3}\big(|\Gamma|_{\hbar,4}^4 - |\Gamma^{\ell-1}|_{\hbar,4}^4\big) \\
&\qquad +\Delta t(\Gamma,\ \Xi-\Xi^{\ell-1})^\hbar \\
&\geq \frac{\Delta t}{2}\big(|\nabla\Gamma|_\hbar^2 - |\nabla\Gamma^{\ell-1}|_\hbar^2\big) + \frac{\Delta t}{2}(|\Xi|_\hbar^2 + |\Xi-\Xi^{\ell-1}|_\hbar^2 - |\Xi^{\ell-1}|_\hbar^2) + \frac{\Delta t}{3}\big(|\Gamma|_{\hbar,4}^4 - |\Gamma^{\ell-1}|_{\hbar,4}^4\big) \\
&\qquad -\frac{\Delta t}{2}|\Gamma|_\hbar^2 - \frac{\Delta t}{2}|\Xi-\Xi^{\ell-1}|_\hbar^2 \\
&\geq \frac{\Delta t}{2}\big(|\nabla\Gamma|_\hbar^2 - |\nabla\Gamma^{\ell-1}|_\hbar^2\big) + \frac{\Delta t}{2}(|\Xi|_\hbar^2 + |\Xi-\Xi^{\ell-1}|_\hbar^2 - |\Xi^{\ell-1}|_\hbar^2) + \frac{\Delta t}{3}\big(|\Gamma|_{\hbar,4}^4 - |\Gamma^{\ell-1}|_{\hbar,4}^4\big) \\
&\qquad -C(|\Psi|,\Delta t) - \frac{\Delta t}{3}|\Gamma|_{\hbar,4}^4 - \frac{\Delta t}{2}|\Xi-\Xi^{\ell-1}|_\hbar^2 \\
&\qquad \geq \beta^2 - C(|\Psi|,\Delta t,\Xi^{\ell-1},\Gamma^{\ell-1}) \geq 0.
\end{aligned} \tag{4.29}$$

Given that Ξ,Γ is a fixed point of the function $\mathcal{G}$, and taking into account (4.22) and (4.1), we deduce that for sufficiently large values of β, the following holds:

$$(\Gamma,\ \Gamma-\Gamma^{\ell-1})^\hbar - (\Xi,\Xi-\Xi^{\ell-1})^\hbar = \frac{-\beta[(A_\Xi(\Xi,\Gamma),\Gamma-\Gamma^{\ell-1})^\hbar - (A_\Gamma(\Xi,\Gamma),\Xi-\Xi^{\ell-1})^\hbar]}{|((A_\Xi(\Xi,\Gamma)),(A_\Gamma(\Xi,\Gamma))|_{\Im^\hbar\times\Im^\hbar}} < 0. \tag{4.30}$$

It follows from (4.23) that

$$\begin{aligned}
(\Gamma,\ \Gamma-\Gamma^{\ell-1})^\hbar - (\Xi,\Xi-\Xi^{\ell-1})^\hbar &\geq |\Gamma|_\hbar^2 - |\Gamma^{\ell-1}|_\hbar^2 + |\Xi|_\hbar^2 - |\Xi^{\ell-1}|_\hbar^2 \\
&= \beta^2 - C(\Xi^{\ell-1},\Gamma^{\ell-1}) \geq 0.
\end{aligned} \tag{4.31}$$

It is evident that (4.1) contradicts (4.30). This contradiction ensures the existence of $\{\Xi,\Gamma\} \in \Im^\hbar \times \Im^\hbar$ such that $A_\Xi(\Xi,\Gamma) = A_\Gamma(\Xi,\Gamma) = 0$. Consequently, this implies the existence of a solution, denoted by $\{\Xi,\Gamma\}$, for the ℓ-th time step of the problem $(\Theta^{\hbar,\Delta t})$. □

5 Numerical results

This section focuses on the numerical analysis of the wave equation. An iterative method has been developed to solve the nonlinear system of equations arising from the problem $(\Theta^{\hbar,\Delta t})$. Furthermore, it presents and analyzes the numerical error results for the Dirichlet non-homogeneous boundary conditions applied to the wave equation in one, two, and three dimensions.

5.1 Numerical algorithm

We begin by outlining a practical algorithm intended to solve the nonlinear algebraic system arising from the approximate problem $(\Theta^{\hbar,\Delta t})$ at each time step:
$(\Theta_i^{\hbar,\Delta t})$: Given $\{\Xi^{\ell,0},\Gamma^{\ell,0}\}\in[\Im^{\hbar}]^2$, then for $\imath\geq 1$ find $\{\Xi^{\ell,\imath},\Gamma^{\ell,\imath}\}\in[\Im^{\hbar}]^2$ such that for all $\Upsilon\in\Im^{\hbar}$

$$\left(\frac{\Xi^{\ell,\imath}-\Xi^{\ell-1}}{\Delta t},\ \Upsilon\right)^{\hbar}+(\nabla\Gamma^{\ell,\imath},\ \nabla\Upsilon)+((\Gamma^{\ell,\imath})^3,\Upsilon)^{\hbar}=0, \tag{5.1}$$

$$\left(\frac{\Gamma^{\ell,\imath}-\Gamma^{\ell-1}}{\Delta t},\ \Upsilon\right)^{\hbar}+(\Gamma^{\ell,\imath},\ \Upsilon)^{\hbar}=(\Xi^{\ell,\imath},\ \Upsilon)^{\hbar}. \tag{5.2}$$

Starting with $\Xi^0\equiv\pi^{\hbar}\xi^0$ and $\Gamma^0\equiv\pi^{\hbar}\gamma^0$, for $\ell\geq 1$, we initialize $\Xi^{\ell,0}\equiv\Xi^{\ell-1}$ and $\Gamma^{\ell,0}\equiv\Gamma^{\ell-1}$. Equations (5.1) and (5.2) can be reformulated into a system of $2\times(J+1)^d$ linear equations by testing (5.1) and (5.2) against the basis functions φ_j, where $j=0,\ldots,J$. For the numerical simulations, we set a tolerance of $TOL=10^{-7}$ and define the stopping criteria based on this tolerance:

$$\max\left\{|\Xi^{\ell,\imath}-\Xi^{\ell,\imath-1}|_{0,\infty},|\Gamma^{\ell,\imath}-\Gamma^{\ell,\imath-1}|_{0,\infty}\right\}<TOL, \tag{5.3}$$

i.e. for $\imath$ fulfilling (5.3) we set $\Xi^{\ell}\equiv\Xi^{\ell,\imath},\Gamma^{\ell}\equiv\Gamma^{\ell,\imath}$.

The programs were implemented in Matlab, and the resulting linear systems were solved employing the Gauss-Seidel iteration method. While a formal proof of the convergence of $\Xi^{\ell,\imath},\Gamma^{\ell,\imath}$ to Ξ^{ℓ},Γ^{ℓ} for a fixed n has not been established, empirical results indicate favorable convergence behaviour. It was observed that the iterative method reliably achieved excellent convergence, typically requiring only a few iterations to fulfill the stopping criteria at each time step.

5.2 Error computations

To assess the error, we make a small modification to the problem (Θ) by adding source terms $f(\mathbf{x},t)$ and $h(\mathbf{x},t)$. This change alters the system described by equations (1.4) and (1.5) into the following form: (Θ) Find $\{\xi,\gamma\}$ such that

$$\partial_t\xi-\Delta\gamma+\gamma^3=f(\mathbf{x},t), \tag{5.4}$$

$$\partial_t\gamma+\gamma-\xi=h(\mathbf{x},t). \tag{5.5}$$

We therefore propose the following fully discrete FEA for $(\Theta_i^{\hbar,\Delta t})$:
$(\Theta_i^{\hbar\ \Delta t})$: Given $\{\Xi^{\ell,0},\Gamma^{\ell,0}\}\in[\Im^{\hbar}]^2$, for $\imath\geq 1$, find $\{\Xi^{\ell,\imath},\Gamma^{\ell,\imath}\}\in[\Im^{\hbar}]^2$ such that for all $\Upsilon\in\Im^{\hbar}$, the following holds:

$$\left(\frac{\Xi^{\ell,\imath}-\Xi^{\ell-1}}{\Delta t},\ \Upsilon\right)^{\hbar}+(\nabla\Gamma^{\ell,\imath},\ \nabla\Upsilon)+((\Gamma^{\ell,\imath})^3,\Upsilon)^{\hbar}=(f(\mathbf{x},t_n),\ \Upsilon), \tag{5.6}$$

$$\left(\frac{\Gamma^{\ell,\imath}-\Gamma^{\ell-1}}{\Delta t},\ \Upsilon\right)^{\hbar}+(\Gamma^{\ell,\imath},\ \Upsilon)^{\hbar}-(\Xi^{\ell,\imath},\ \Upsilon)^{\hbar}=(h(\mathbf{x},t_n),\ \Upsilon). \tag{5.7}$$

5.2.1 One-dimensional error

This section presents two numerical examples that solve the system described by equations (5.6) and (5.7) under homogeneous Dirichlet boundary conditions and specified initial conditions. For simplicity, all examples are conducted with the spatial domain $\Psi=[0,1]$ and a time period of $T=1$. The initial and boundary conditions, as well as the source terms $f(x,t)$ and $h(x,t)$, are chosen according to the specific exact solution for each case. Initially, the domain $\Psi=[0,1]$ is uniformly divided into J intervals to form a square mesh. The mesh size for each element is represented as $h=1/J$, and $\Delta t=10^{-4}$. The exact solutions are given by:

$$\gamma(x,t)=\sin(2\pi x)\exp(-2t).$$

The errors in the L^1, L^2, and L^∞ norms are presented in Table 1.

J	L^1	L^2	L^∞
100	1.02E-02	3.69E-03	1.41E-02
200	2.39E-03	5.99E-04	3.60E-03
250	1.52E-03	3.38E-04	2.29E-03
400	5.78E-04	1.02E-04	8.87E-04
500	3.66E-04	5.76E-05	5.64E-04
600	8.73E-05	9.70E-06	1.36E-04

Table 1: Discrete L^1, L^2, L^∞-norms error

J	L^1	L^2	L^∞
100	1.02E-02	1.34E-03	1.96E-02
200	2.46E-03	1.55E-04	5.58E-03
250	1.57E-03	7.77E-05	3.57E-03
400	5.96E-04	1.85E-05	1.40E-03
500	3.78E-04	9.36E-06	8.96E-04
600	9.35E-05	1.15E-06	2.26E-04

Table 2: Discrete L^1, L^2, L^∞-norms error

5.2.2 Two-dimensional error

In a two-dimensional scenario governed by the system described by equations (5.6) and (5.7) with Dirichlet boundary conditions and an initial condition, the spatial domain is confined to $\Psi = [0,1] \times [0,1]$. The time interval is specified as $[0,T] = [0,1]$ for simplicity in analysis. The initial and boundary conditions, together with the source terms $f(x,y,t)$ and $h(x,y,t)$, should be selected to align with the specific exact solution relevant to each case. The chosen time step for the simulations is $\Delta t = 10^{-4}$. The exact solution is:

$$\gamma(x,y,t) = \sin(2\pi x)\sin(2\pi y)\exp(-2t)$$

The errors in the L^1, L^2, and L^∞-norms for this simulations are listed in Table 2.

5.2.3 Three-dimensional error

In this section, we present a three-dimensional example, considering the system described by (5.6) and (5.7) with Dirichlet boundary and initial conditions. For this numerical example, we simplify the spatial domain to $\Psi = [0,1] \times [0,1] \times [0,1]$, with the time interval set to $[0,T] = [0,1]$. The initial and boundary conditions, as well as the source terms $f(x,y,z,t)$ and $h(x,y,z,t)$, will be defined according to the specific exact solution for each case. The time step is selected as $\Delta t = 10^{-4}$. The exact solution is given by:

$$\gamma(x,y,z,t) = \sin(2\pi x)\sin(2\pi y)\sin(2\pi z)\exp(-2t).$$

The errors in the L^1, L^2, and L^∞-norms for this simulations are provided in Table 3.

J	L^1	L^2	∞
100	2.39E-03	1.15E-04	6.41E-03
200	3.49E-04	5.48E-06	1.19E-03
250	2.05E-04	2.26E-06	7.05E-04
400	6.83E-05	3.73E-07	2.48E-04
500	4.11E-05	1.60E-07	1.51E-04
600	7.41E-06	1.02E-08	2.82E-05

Table 3: Discrete L^1, L^2, L^∞-norms error

6 Numerical simulations

6.1 One-dimensional simulations

This section is dedicated to the approximated solution of the DWE with Neumann boundary conditions in a one-dimensional space.

Example 6.1. *We solve the one-dimensional wave equation with the following initial conditions:*

$$\gamma(x,0) = \sin(2\pi x), \qquad \gamma_t(x,0) = 0.5\sin(2\pi x), \qquad x \in [0,1]. \tag{6.1}$$

The approximated solution to this equation was computed employing $\Delta t = 0.00001$ and $J = 200$. Figure 1 shows the approximated solutions at various time instances.

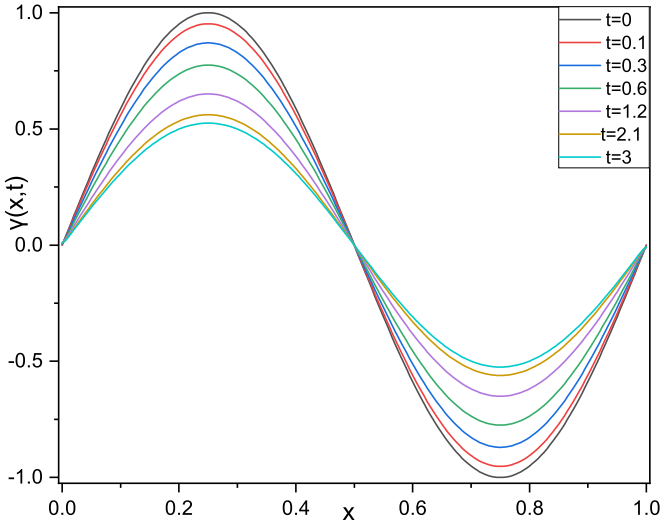

Figure 1: Numerical solution at $T = 3$, with $\Delta t = 0.00001 \quad and \quad J = 200$.

6.2 Two-dimensional simulations

In this section, we focus on the approximated solution of the DWE with Neumann boundary conditions in two-dimensional space.

Example 6.2. *We investigate the two-dimensional wave equation with the following initial conditions:*

$$\gamma(x,y,0) = \sin(2\pi x)\sin(2\pi y), \quad \gamma_t(x,y,0) = 0.5\sin(2\pi x)\sin(2\pi y), \quad (x,y) \in [0,1]\times[0,1]. \tag{6.2}$$

We solve this model with $t = 0.000001$ and $J = 20$. Figure 2 shows the plot of the approximated solution $\gamma(x,y)$ at $T = 0.1$.

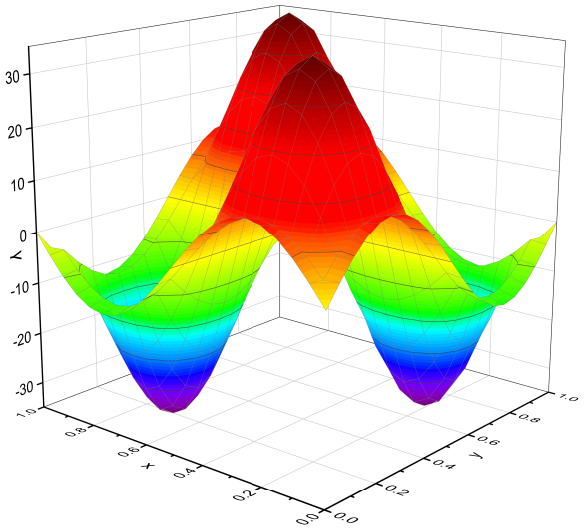

Figure 2: Numerical solution at $T = 0.1$, with $\Delta t = 0.000001 \quad and \quad J = 20$.

7 Conclusions

This study delves into the numerical analysis of the DWE on open bounded convex domains $\mathfrak{R} \subset \mathbb{R}^d$, where $d \leq 3$, under Neumann boundary conditions. We propose two numerical solutions, which are SDA and FDA. The existence and uniqueness of solutions for both schemes are established. Our findings indicate a first-order error rate in the temporal discretisation and a second-order error rate in the spatial discretisation, applicable in both one- and two-dimensional cases. Moreover, we derive multiple bounds for the approximate solutions across different function spaces. The paper also includes a practical algorithm for solving the approximate problem, which is utilized to generate numerical results. This framework provides deeper insights into the solution's behaviour and supports its practical implementation.

The impact of mesh size on the accuracy of the FEM is a crucial factor in numerical simulations. Reducing the mesh size generally improves the FEM solution, as it converges towards the exact solution or a more precise approximation an attribute known as the convergence property of FEM. Finer mesh elements provide a more detailed representation of the geometry and physical phenomena, enhancing accuracy. However, FEM inherently presents discretisation error due to the approximation of continuous functions with piecewise polynomial ones. This

error decreases as the mesh size becomes smaller, leading to a more accurate solution. Additionally, smaller mesh elements are better at capturing local variations, particularly in areas with steep gradients or abrupt changes in the solution, thereby "smoothing out" the results.

Despite these benefits, smaller mesh elements significantly increase the computational cost. A finer mesh involves a larger number of elements, which translates to solving a more extensive system of equations, requiring additional computational time and memory. Thus, selecting an optimal mesh size is essential in FEM simulations, balancing accuracy and computational efficiency. Refining the mesh is often an effective strategy to enhance accuracy, but adaptive meshing techniques and consideration of the problem's specific features can yield more efficient and tailored solutions.

Acknowledgments

We are grateful to the anonymous reviewer whose insightful comments greatly contributed to improving the quality of this manuscript.

References

[1] Al-Juaifri, G. A. and Harfash, A. J. (2023). Finite element analysis of nonlinear reaction–diffusion system of Fitzhugh–Nagumo type with Robin boundary conditions. Mathematics and Computers in Simulation, 203:486–517.

[2] Al-Musawi, G. A. and Harfash, A. J. (2024a). Finite element analysis of extended fisher-kolmogorov equation with neumann boundary conditions. Applied Numerical Mathematics, 201:41–71.

[3] Al-Musawi, G. A. and Harfash, A. J. (2024b). Finite element approximation of coupled cahn-hilliard equations with a logarithmic potential and nondegenerate mobility. Journal of Mathematical Modeling, 13(1):49–68.

[4] Ball, J. (1978). On the asymptotic behavior of generalized processes, with applications to nonlinear evolution equations. Journal of differential equations, 27(2):224–265.

[5] Ball, J. M. (2004). Global attractors for damped semilinear wave equations. Discrete and Continuous Dynamical Systems, 10(1/2):31–52.

[6] Ciarlet, P. G. (2002). The Finite Element Method for Elliptic Problems. SIAM.

[7] Ciarlet, P. G. and Raviart, P.-A. (1972). General lagrange and hermite interpolation in R^n with applications to finite element methods. Archive for Rational Mechanics and Analysis, 46(3):177–199.

[8] Ciavaldini, J. (1975). Analyse numerique dun problème de stefan à deux phases par une methode delements finis. SIAM Journal on Numerical Analysis, 12(3):464–487.

[9] Cohen, G., Joly, P., Roberts, J. E., and Tordjman, N. (2001). Higher order triangular finite elements with mass lumping for the wave equation. SIAM Journal on Numerical Analysis, 38(6):2047–2078.

[10] Cox, S. J. and Overton, M. L. (1996). Perturbing the critically damped wave equation. SIAM Journal on Applied Mathematics, 56(5):1353–1362.

[11] Dehghan, M. (2005a). Efficient techniques for the second-order parabolic equation subject to nonlocal specifications. Applied Numerical Mathematics, 52(1):39–62.

[12] Dehghan, M. (2005b). On the solution of an initial-boundary value problem that combines neumann and integral condition for the wave equation. Numerical Methods for Partial Differential Equations, 21(1):24–40.

[13] Dehghan, M. (2006a). Finite difference procedures for solving a problem arising in modeling and design of certain optœlectronic devices. Mathematics and Computers in Simulation, 71(1):16–30.

[14] Dehghan, M. (2006b). Solution of a partial integro-differential equation arising from viscœlasticity. International Journal of Computer Mathematics, 83(1):123–129.

[15] Ern, A. and Guermond, J.-L. (2013). Theory and practice of finite elements, volume 159. Springer Science & Business Media.

[16] Fan, L., Liu, H., and Zhao, H. (2013). One-dimensional damped wave equation with large initial perturbation. Analysis and Applications, 11(04):1350013.

[17] Grote, M. J. and Schötzau, D. (2009). Optimal error estimates for the fully discrete interior penalty dg method for the wave equation. Journal of Scientific Computing, 40(1):257–272.

[18] Hashim, M. H. and Harfash, A. J. (2021). Finite element analysis of a Keller–Segel model with additional cross-diffusion and logistic source. part I: Space convergence. Computers and Mathematics with Applications, 89(1):44–56.

[19] Hashim, M. H. and Harfash, A. J. (2022a). Finite element analysis of a Keller-Segel model with additional cross-diffusion and logistic source. part II: Time convergence and numerical simulation. Computers and Mathematics with Applications, 109(1):216–234.

[20] Hashim, M. H. and Harfash, A. J. (2022b). Finite element analysis of attraction-repulsion chemotaxis system. Part I: Space convergence. Communications on Applied Mathematics and Computation, 4(3):1011–1056.

[21] Hashim, M. H. and Harfash, A. J. (2022c). Finite element analysis of attraction-repulsion chemotaxis system. Part II: Time convergence, error analysis and numerical results. Communications on Applied Mathematics and Computation, 4(3):1057–1104.

[22] Hashim, M. H. and Harfash, A. J. (2024a). Finite element analysis for microscale heat equation with neumann boundary conditions. Iranian Journal of Numerical Analysis and Optimization, 14(3):796–832.

[23] Hashim, M. H. and Harfash, A. J. (2024b). The convergence of the finite element approximation to the weak solution of attraction-repulsion chemotaxis system with additional self-diffusion term. Journal of Mathematical Sciences, pages 1–50.

[24] Hassan, S. M. and Harfash, A. J. (2022a). Finite element analysis of a two-species chemotaxis system with two chemicals. Applied Numerical Mathematics, 182:148–175.

[25] Hassan, S. M. and Harfash, A. J. (2022b). Finite element analysis of the two-competing-species Keller–Segel chemotaxis model. Computational Mathematics and Modeling, 33(4):443–471.

[26] Hassan, S. M. and Harfash, A. J. (2022c). Finite element approximation of a Keller–Segel model with additional self-and cross-diffusion terms and a logistic source. Communications in Nonlinear Science and Numerical Simulation, 104:106063.

[27] Hassan, S. M. and Harfash, A. J. (2023). Finite element analysis of chemotaxis-growth model with indirect attractant production and logistic source. International Journal of Computer Mathematics, 100(4):745–774.

[28] Holden, H., Karlsen, K., and Risebro, N. (2009). A convergent finite-difference method for a nonlinear variational wave equation. IMA journal of numerical analysis, 29(3):539–572.

[29] Hosono, T. and Ogawa, T. (2004). Large time behavior and $L^p - L^q$ estimate of solutions of 2-dimensional nonlinear damped wave equations. Journal of differential equations, 203(1):82–118.

[30] Jean-Luc Guermond, A. (2004). Theory and practice of finite elements.

[31] Jenkins, E. W., Rivière, B., and Wheeler, M. F. (2002). A priori error estimates for mixed finite element approximations of the acoustic wave equation. SIAM Journal on Numerical Analysis, 40(5):1698–1715.

[32] Johnson, C. (1993). Discontinuous galerkin finite element methods for second order hyperbolic problems. Computer Methods in Applied Mechanics and Engineering, 107(1-2):117–129.

[33] Karaa, S. (2011). Error estimates for finite element approximations of a viscous wave equation. Numerical functional analysis and optimization, 32(7):750–767.

[34] Karaa, S. (2012). Stability and convergence of fully discrete finite element schemes for the acoustic wave equation. Journal of Applied Mathematics and Computing, 40:659–682.

[35] Karch, G. (2000). Selfsimilar profiles in large time asymptotics of solutions to damped wave equations. Studia Mathematica, 2(143):175–197.

[36] Larsson, S., Thomée, V., and Wahlbin, L. B. (1991). Finite-element methods for a strongly damped wave equation. IMA journal of numerical analysis, 11(1):115–142.

[37] Lin, J. and Zhai, J. (2012). Blow-up of the solution for semilinear damped wave equation with time-dependent damping. Communications in Contemporary Mathematics, 14(05):1250034.

[38] Matsuo, T. (2007). New conservative schemes with discrete variational derivatives for nonlinear wave equations. Journal of computational and applied mathematics, 203(1):32–56.

[39] Mickens, R. E. and Jordan, P. (2004). A positivity-preserving nonstandard finite difference scheme for the damped wave equation. Numerical Methods for Partial Differential Equations, 20(5):639–649.

[40] Narazaki, T. (2004). $L^p - L^q$ estimates for damped wave equations and their applications to semi-linear problem. Journal of the Mathematical Society of Japan, 56(2):585–626.

[41] Nishiyama, H. (2015). Remarks on the asymptotic behavior of the solution of an abstract damped wave equation. arXiv preprint arXiv:1505.01794.

[42] Rincon, M. and Copetti, M. (2013). Numerical analysis for a locally damped wave equation. Journal of Applied Analysis & Computation, 3(2):169–182.

[43] Shang, Y. (2000). Blow-up of solutions for two classes of strongly damped nonlinear wave equations. Journal of Engineering Mathematics, 17(2):65–70.

[44] Shubov, M. A. (1998). Exact boundary and distributed controllability of radial damped wave equation. Journal de mathématiques pures et appliquées, 77(5):415–437.

[45] Wang, S. and An, Y. (2011). Multiple periodic solutions to a suspension bridge wave equation with damping. International Scholarly Research Notices, 2011(1):154806.

[46] Ye, Y. (2015). Global existence and blow-up of solutions for higher-order viscœlastic wave equation with a nonlinear source term. Nonlinear Analysis: Theory, Methods and Applications, 112:129–146.